

AD-A172 894

INFORMATION ON THE IMPACT PARAMETER DEPENDENCE OF THE
BAI YIELDS BAI(U-S)+N REACTION(U) STANFORD UNIV CA DEPT
OF CHEMISTRY C NODA ET AL. 15 JUL 86 AFOSR-IR-86-1826
F49628-85-C-0021 P/G 7/4

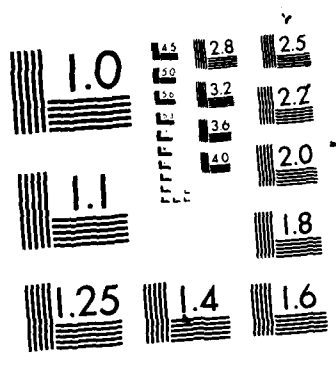
1/1

UNCLASSIFIED

NL



END
DATE
FILMED
12-86
F T



MICROCOPY RESOLUTION TEST CHART
NATIONAL BUREAU OF STANDARDS 1963-A

AD-A172 894

DTIC
ELECTE
OCT 17 1986
S B

DISTRIBUTION STATEMENT A
Approved for public release
Distribution Unlimited

UNCLASSIFIED

AUG 18 1986

8/28

SECURITY CLASSIFICATION OF THIS PAGE

REPORT DOCUMENTATION PAGE

1a. REPORT SECURITY CLASSIFICATION UNCLASSIFIED		1b. RESTRICTIVE MARKINGS	
2a. SECURITY CLASSIFICATION AUTHORITY		3. DISTRIBUTION/AVAILABILITY OF REPORT Approved for public release; distribution unlimited	
2b. DECLASSIFICATION/DOWNGRADING SCHEDULE			
4. PERFORMING ORGANIZATION REPORT NUMBER(S)		5. MONITORING ORGANIZATION REPORT NUMBER(S) AFOSR-TR. 86-1026	
6a. NAME OF PERFORMING ORGANIZATION Professor Richard N. Zare	6b. OFFICE SYMBOL (If applicable)	7a. NAME OF MONITORING ORGANIZATION AFOSR	
6c. ADDRESS (City, State and ZIP Code) Department of Chemistry Stanford University Stanford, CA 94305		7b. ADDRESS (City, State and ZIP Code) Bldg 410 Bolling AFB DC 20332	
8a. NAME OF FUNDING/SPONSORING ORGANIZATION U. S. Army Research Office	8b. OFFICE SYMBOL (If applicable) NC	9. PROCUREMENT INSTRUMENT IDENTIFICATION NUMBER AFOSR F49620-85-C-0021	
8c. ADDRESS (City, State and ZIP Code) P. O. Box 12211 Research Triangle Park, NC 27709		10. SOURCE OF FUNDING NOS.	
11. TITLE (Include Security Classification) "Information on the Impact..Reaction."		PROGRAM ELEMENT NO. 61102F	PROJECT NO. 2303
12. PERSONAL AUTHOR(S) NODA/McKILLOP/JOHNSON/WALDECK/ZARE		TASK NO. B1	WORK UNIT NO.
13a. TYPE OF REPORT Interim	13b. TIME COVERED FROM _____ TO _____	14. DATE OF REPORT (Yr., Mo., Day) 8/12/86	15. PAGE COUNT 46
16. SUPPLEMENTARY NOTATION The view, opinions, and/or findings contained in this report are those of the author(s) and should not be construed as an official Department of the Army position, policy, or decision.			
17. COSATI CODES		18. SUBJECT TERMS (Continue on reverse if necessary and identify by block number)	
FIELD	GROUP	SUB. GR.	
19. ABSTRACT (Continue on reverse if necessary and identify by block number) <p style="text-align: center;">SEE REVERSE SIDE</p>			
20. DISTRIBUTION/AVAILABILITY OF ABSTRACT UNCLASSIFIED/UNLIMITED <input checked="" type="checkbox"/> SAME AS RPT <input type="checkbox"/> DTIC USERS <input type="checkbox"/>		21. ABSTRACT SECURITY CLASSIFICATION UNCLASSIFIED	
22a. NAME OF RESPONSIBLE INDIVIDUAL Professor Richard N. Zare		22b. TELEPHONE NUMBER (Include Area Code) 415/497-3062	22c. OFFICE SYMBOL

ABSTRACT

Using selectively detected laser-induced fluorescence, the rotational state distribution of the BaI product has been measured for the beam-gas reaction, $\text{Ba} + \text{HI} \rightarrow \text{BaI}(\nu=8) + \text{H}$. Owing to the highly constrained kinematics for this system, these measurements can be used to derive the reaction probability as a function of the impact parameter for this channel, called the "specific" opacity function, once the reaction probability as a function of velocity has been determined. Unfortunately, lack of knowledge of the exoergicity, and the height of any energy barrier prevents a conclusive determination of the specific opacity function for this reaction. Instead, various approximate opacity functions are estimated based on different models of the velocity dependence of the reaction channel studied. If the reaction probability is the same for all relative collision velocities, then the BaI($\nu=8$) specific opacity function peaks strongly near 2.6 Å with a full width at half maximum of 1.0 Å. However, the possible presence of a small energy barrier in the entrance channel causes a cutoff in the relative collision velocity distribution, and this type of velocity dependence would significantly affect the shape of the specific opacity function.

Information on the impact parameter dependence of the Ba + HI → BaI($\nu = 8$) + H reaction

Chifuru Noda, John S. McKillop,^{a)} Mark A. Johnson,^{b)} Janet R. Waldeck, and Richard N. Zare

Department of Chemistry, Stanford University, Stanford, California 94305

(Received 12 September 1985; accepted 11 April 1986)

Using selectively detected laser-induced fluorescence, the rotational state distribution of the BaI product has been measured for the beam-gas reaction Ba + HI → BaI($\nu = 8$) + H. Owing to the highly constrained kinematics for this system, these measurements can be used to derive the reaction probability as a function of the impact parameter for this channel, called the "specific opacity function," once the reaction probability as a function of velocity has been determined. Unfortunately, lack of knowledge of the exoergicity and the height of any energy barrier prevents a conclusive determination of the specific opacity function for this reaction. Instead, various approximate opacity functions are estimated based on different models of the velocity dependence of the reaction channel studied. If the reaction probability is the same for all relative collision velocities, then the BaI($\nu = 8$) specific opacity function peaks strongly near 2.6 Å with a full width at half-maximum of 1.0 Å. However, the possible presence of a small energy barrier in the entrance channel causes a cutoff in the relative collision velocity distribution, and this type of velocity dependence would significantly affect the shape of the specific opacity function.

I. INTRODUCTION

Consider the elementary reaction



where A, B, and C are atoms and ν denotes the vibrational state. Although the AB product is often detected independent of the vibrational state, the use of laser spectroscopic techniques allows experimentalists to study the reaction channel for an individual product vibrational state. Regardless of whether a specific vibrational state is detected, contemporary experimental studies of reaction dynamics tend to ignore the detailed dependence of the reaction probability on the impact parameter b , which is defined as the distance of closest approach of the incoming reagents if they move in undeflected straight lines.^{1,2} This is primarily a consequence of the fact that experimentalists cannot control the choice of the impact parameter in a collision.

The impact parameter is related to the cross section, $\sigma_\nu(v_{rel})$, for reaction (1) by

$$\sigma_\nu(v_{rel}) = 2\pi \int_0^\infty P_\nu(b, v_{rel}) b db, \quad (2)$$

where $P_\nu(b, v_{rel})$ gives the reaction probability for a given v_{rel} and b to produce the AB product in a specific vibrational level, ν (averaged over all reagent orientations). Thus, $P_\nu(b, v_{rel})$ is called a "specific" opacity function, which must be distinguished from the "overall" opacity function $P(b, v_{rel})$. This overall opacity function describes the reaction probability for a given v_{rel} and b to produce the AB product in any vibrational state, and is related to the specific opacity functions by

$$P(b, v_{rel}) = \sum_\nu P_\nu(b, v_{rel}). \quad (3)$$

The "velocity-averaged" specific opacity function is then defined as

$$P_\nu(b) = \int_0^\infty P_\nu(b, v_{rel}) f(v_{rel}) dv_{rel} / \int_0^\infty f(v_{rel}) dv_{rel}, \quad (4)$$

where $f(v_{rel})$ is the relative velocity distribution of the reagents in the center of mass collision frame. In terms of $P_\nu(b)$, the velocity-averaged cross section σ_ν is related to the specific opacity function by

$$\sigma_\nu = 2\pi \int_0^\infty P_\nu(b) b db. \quad (5)$$

As first pointed out by Herschbach,³ under certain favorable circumstances it is possible to remove the seemingly intrinsic average over b and glimpse the detailed role of the impact parameter in governing the outcome of a reactive encounter. The key is to choose a kinematically constrained reaction, for example, that of a heavy atom plus a heavy-light diatomic reacting to give a heavy-heavy diatomic product plus a light escaping atom.^{3,4} A near limiting example of such a reaction is



As a consequence of the conservation of angular momentum, nearly all of the reagent angular momentum L is channeled into rotational angular momentum J of the diatomic product. Here $|L| = \mu v_{rel} b$, where for reaction (6),

$$1/\mu = 1/m_{Ba} + 1/m_{HI}. \quad (7)$$

Thus, for a given v_{rel} , the distribution of the reactive impact parameters is mapped into the population of the product rotational levels through the relation

$$|J| = |L| = \mu v_{rel} b. \quad (8)$$

Although this possibility of determining the specific

^{a)} Thomas J. Watson Research Center, IBM, Yorktown Heights, NY 10598.

^{b)} Department of Chemistry, Yale University, New Haven, CT 06510.

opacity function for kinematically constrained systems was proposed more than 20 years ago,³ there has been no attempt to carry out the actual measurements to date. This is mainly due to the fact that the reaction product must be, by definition, a heavy molecule, and consequently, the spectra are very congested, hindering a rotational analysis. We present here the first experimental measurement of the product rotational distribution for the $\text{Ba} + \text{HI} \rightarrow \text{BaI}(\nu = 8) + \text{H}$ system, and use this information to estimate the specific opacity function for this reaction channel, assuming various models for the dependence of the reaction probability on relative collision velocity.

When the relative velocity distribution has some spread, the product rotational population is affected by the velocity dependence of the reaction probability. This velocity dependence can be separated into (a) the probability that a trajectory reaches a transition state, and (b) the probability that a reaction takes place after a trajectory has reached a transition state. We call the former a "transmission" velocity dependence, and the latter an "intrinsic" velocity dependence. The transmission velocity dependence is caused by the existence of an activation energy barrier in the entrance channel and by the energetics of the reaction, both of which permit only velocities greater than some threshold to react to produce the BaI product in $\nu = 8$. The intrinsic velocity dependence arises from, for instance, a decrease in the interaction time between the reagents at high collision velocities (see pp. 116–118 of Ref. 2).

As will be discussed in Sec. III, the lack of information on the exoergicity, the height of the energy barrier, and the intrinsic velocity dependence of the reaction probability prohibits a unique determination of the specific opacity function for this reaction system. This implies that the relative distribution in product rotation $P(J)$ can only be related to the specific opacity function $P_\nu(b)$ with assumed forms of the velocity dependence.

II. EXPERIMENTAL

The experimental apparatus used in this work has been described elsewhere,^{5–7} and the experimental techniques employed here are explained in detail in Ref. 7. Thus only a brief account is provided here. The vacuum chamber consists of two differentially pumped chambers: one for the Ba beam source, the other for the beam-gas reaction. The pressure is measured using uncalibrated Bayard-Alpert type ionization gauges. A typical base pressure is 1×10^{-6} Torr. A stainless steel crucible containing Ba metal (purity 99.5%, Alfa Products) has an orifice of 0.4 mm diameter and is radiatively heated to 985 °C. Before each experiment, HI gas (purity 98.0%, Matheson) was cooled to liquid N₂ temperature and pumped to remove H₂, which is always present due to the equilibrium $2\text{HI} \rightleftharpoons \text{H}_2 + \text{I}_2$. During the experiments, the temperature of the HI cylinder is kept at -20 °C to condense I₂. At this temperature, the HI pressure is on the order of one atmosphere,⁸ and the HI gas is introduced into the reaction chamber via a double-needle precision valve. The HI pressure in the reaction chamber is maintained at 2.0×10^{-4} Torr (uncalibrated ionization gauge reading).

A single-mode ring dye laser (Spectra-Physics 380D) is pumped by the 514.5 nm line of an Ar⁺ laser (Coherent CR-18). Rhodamine 560 dye is used with a pH = 10 buffer solution to prolong dye lifetime. The typical output power is 200 mW with a 4 W pump laser power. The laser beam intersects the Ba beam at right angles. The resulting fluorescence is monitored by a cooled photomultiplier (Centronics Q4283RA, extended S-20 photocathode) through a 1 m monochromator (Interactive Technology) equipped with a 1200 grooves/mm grating, and measured by a standard photon counter-rate meter combination. A YAG-pumped dye laser (Quanta-Ray DCR-1A/PDL-1) was used to obtain broadband excitation spectra, as shown in Fig. 1. The spectrum shown in Fig. 1 is similar to the one reported by Cruse,

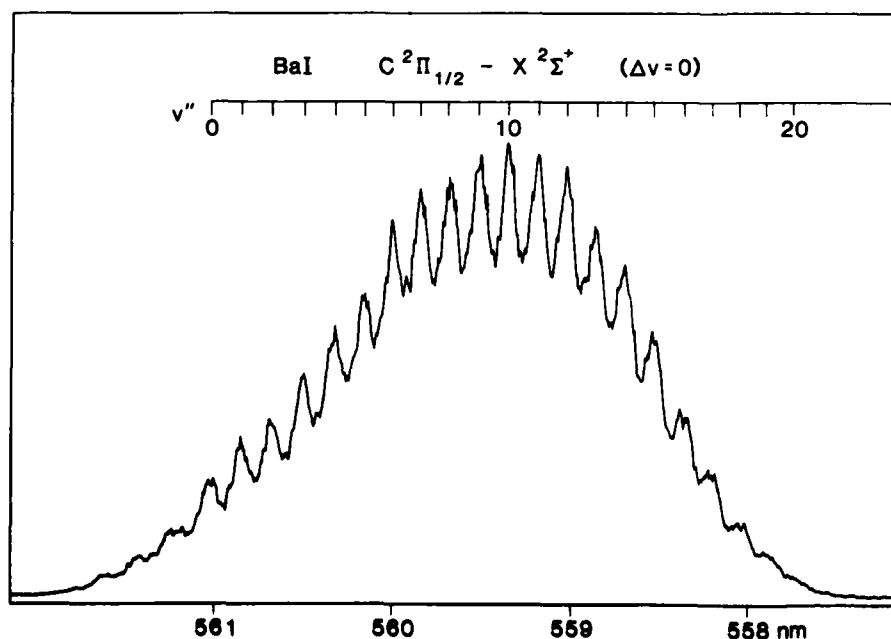


FIG. 1. A low-resolution excitation spectrum of the BaI $C^2\Pi_{1/2} - X^2\Sigma^+$ system, using a YAG-pumped dye laser with a bandwidth of ~ 0.3 cm^{-1} . Since the Franck-Condon factors for $\Delta v = 0$ transitions are almost unity and all the transitions are strongly saturated, the intensities of the transitions give rough estimates of the product vibrational populations.

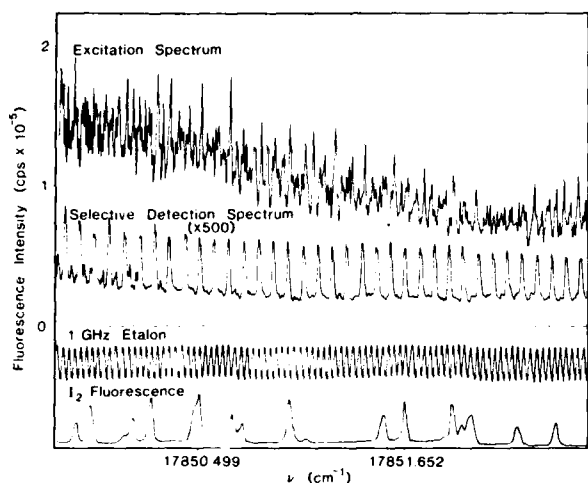


FIG. 2. A 3 cm^{-1} segment of the $\text{BaI } C^2\Pi_{1/2}-X^2\Sigma^+$ (8,8) excitation spectrum (upper trace) and the selectively detected laser-induced fluorescence spectrum (middle trace). An I_2 fluorescence spectrum and 1 GHz etalon markers, which were used to calibrate wavelengths, are shown in the lower two traces.

Dagdigan, and Zare,⁹ who first studied this reaction under crossed jet conditions.

While the large mass of the heavy-heavy product is required for a rigorous kinematic constraint on the reaction $\text{Ba} + \text{HI} \rightarrow \text{BaI} + \text{H}$, it also causes the visible spectra of the BaI product to be congested and hence difficult to analyze.^{6,10} For example, only bandheads and rotational contours can be resolved in the BaI product excitation spectrum observed in the beam-gas reaction $\text{Ba} + \text{HI}$ using a pulsed dye laser with $\sim 0.3 \text{ cm}^{-1}$ bandwidth (see Fig. 1). When a single-mode dye laser with a bandwidth narrower than the natural linewidth of the BaI $C^2\Pi$ state is used, the excitation spectrum (upper trace of Fig. 2) is too congested to permit an accurate measurement of the rotational distribution or

even an assignment of the lines in many cases. The small rotational constants of the upper and lower states of the $C^2\Pi-X^2\Sigma^+$ band system ($B' \approx B'' \approx 0.027 \text{ cm}^{-1}$, Ref. 6) combined with the Rydberg character of the upper state that places its potential almost directly above and nearly parallel to the ground state potential conspire to produce this congestion. It might appear then that the unambiguous measurement of a product state distribution for this reaction would be impossible. We have, however, succeeded in carrying out a rotational analysis^{6,7,10,11} using a combination of laser techniques, in particular optical-optical double resonance and selectively detected laser induced fluorescence (SDLIF).¹² The latter method is of particular use and deserves discussion here.

Figure 3 shows a Fortrat diagram illustrating the SDLIF technique for the $\text{BaI } C^2\Pi_{1/2}-X^2\Sigma^+$ subband. The six possible rotational transitions in this subband can be separated into two groups according to the parity component (Λ doublet) of the $^2\Pi$ excited state. Thus excitation via the P_{12} branch results in fluorescence in the P_{12} , Q_1 , and R_{12} branches. If a monochromator isolates the fluorescence of the $Q_1 + R_{12}$ bandhead, it is thus possible to detect selectively excitation of individual rotational transitions in the P_{12} branch. Figure 2 presents a 3 cm^{-1} segment of the BaI $C-X$ excitation spectrum (upper trace) and the selectively detected fluorescence spectrum (middle trace) for the rotational levels of the $\text{BaI} (\nu = 8)$ product observed in the $\text{Ba} + \text{HI}$ beam-gas reaction. Note that the rotational distribution is so extensive that it still appears flat, even when over 35 rotational levels were observed, as in this scan.

Since selective detection relies on isolation of fluorescence, it is mandatory to narrow the monochromator slits, typically, to $150 \mu\text{m}$. This unfortunately causes the detection sensitivity of P_{12} excitation to vary as a function of J , since the frequency of the $Q_1 + R_{12}$ transition changes and the "slit function" of the monochromator is not constant over the $Q_1 + R_{12}$ bandhead. This problem was overcome by a direct measurement of the slit function. When an experiment

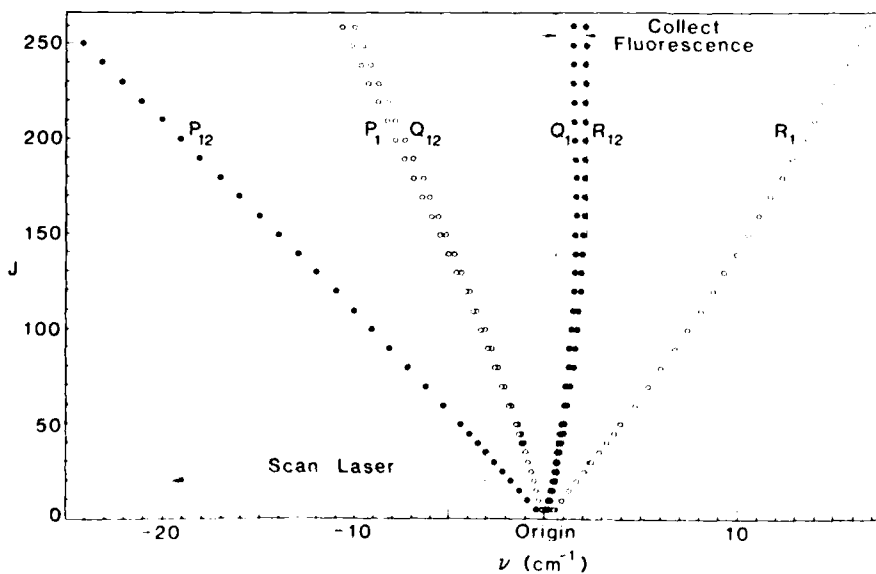


FIG. 3. A Fortrat diagram of the $\text{BaI } C^2\Pi_{1/2}-X^2\Sigma^+$ system. Closed dots represent transitions involving f level upper states (Λ -doubling components), and open dots represent transitions involving e level upper states. When a monochromator collects fluorescence only in the $Q_1 + R_{12}$ bandhead region, the excitation of the P_{12} transitions can be selectively detected.

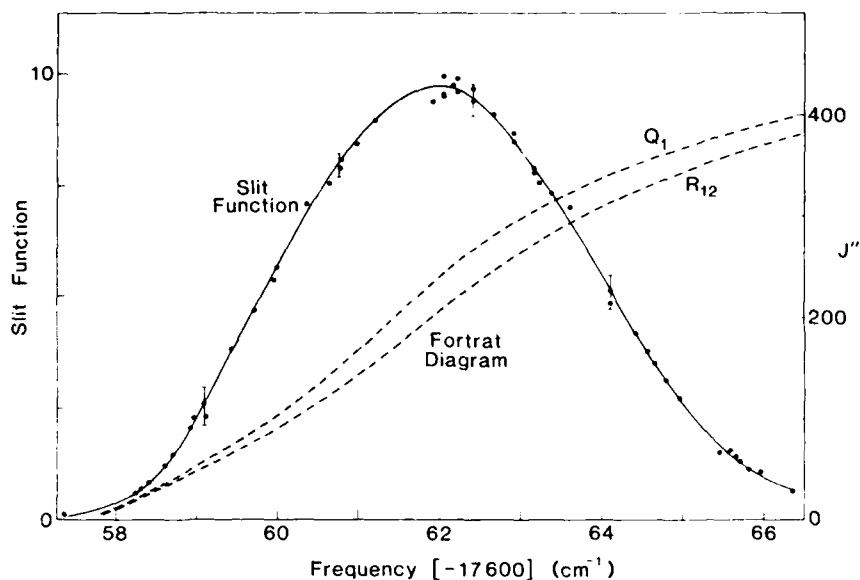


FIG. 4. The experimentally observed slit function and line positions of the BaI C-X(8,8) Q_1 and R_{12} transitions.

is completed, N_2 gas is introduced into the reaction chamber and scattered light from the laser is measured as the laser scans across the slit function. The scattered light intensity divided by the laser power gives the slit function of the particular experiment's monochromator setting (see Fig. 4). The detection efficiency for the $P_{12}(J)$ transition $D(J)$ is then given by

$$D(J) = S[Q_1(J-1)] \times [\text{slit function at } Q_1(J-1)] \\ + S[R_{12}(J-2)] \times [\text{slit function at } R_{12}(J-2)], \quad (9)$$

where S denotes the line strength for the transition in parentheses divided by $2J+1$ and the slit function is evaluated at the frequency of the transition, as shown in Fig. 4. Since we are interested only in the relative intensities, the ratios of the line strengths are used in Eq. (9): 2 for members of the Q_1 branch, and 1 for members of the R_{12} branch (the high- J limiting ratios).¹³

The BaI product will have the rotational alignment, defined as $\langle P_2(\hat{\mathbf{J}} \cdot \hat{\mathbf{v}}_{\text{rel}}) \rangle$ ¹⁴ where $\hat{\mathbf{J}} \cdot \hat{\mathbf{v}}_{\text{rel}}$ is the cosine of the angle between the product rotational angular momentum \mathbf{J} and the reagent relative velocity vector \mathbf{v}_{rel} , $P_2(x) = (3 \cos^2 x - 1)/2$, and the superscript caret denotes a unit vector. Because of the kinematic constraint, the product rotational angular momentum is equal to the reagent orbital angular momentum $\mathbf{J} = \mathbf{L}$ and consequently \mathbf{J} is perpendicular to \mathbf{v}_{rel} regardless of the magnitude of the angular momentum. Hence, the rotational alignment is independent of J and the effect of the product alignment on the detection sensitivity of each rotational state can be neglected.

The BaI $C^2\Pi-X^2\Sigma^+$ band system is known to be saturated very easily.^{15,16} This could be avoided by using a very low laser power at a sacrifice of signal intensity. We adopted, however, a different approach. The unattenuated laser is used to nearly saturate the transition and the laser power is recorded at the same time as the SDLIF spectra are taken.

Later, the dependence of the signal intensity on the laser power is measured, and the signals are corrected accordingly (see Fig. 5). It is important to note that, since the laser power is very high and the transition is strongly saturated, the laser-induced fluorescence method functions in this instance neither as a density detector nor as a flux detector, but as some intermediate between the two.¹⁶ Fortunately the correlation between v_{rel} and v_{CM} is very weak in the Ba + HI beam-gas reaction, so that the resulting relative distributions become, within the experimental error, the same whether detected as a flux or as a density.

Recalling that $|\mathbf{J}| = \mu v_{\text{rel}} b$, it is important to determine v_{rel} and, therefore, to know the velocity distributions of Ba and HI. The HI velocity can be assumed to follow the Maxwell-Boltzmann distribution. The Ba beam velocity is measured directly using a Doppler-shift method,¹⁷ which employs two laser beams, one intersecting the Ba beam at right angles and the other at 45° . When the laser is scanned across the Ba atomic line profile ($^1P^\circ - ^1S_0$ at $18\,060.264 \text{ cm}^{-1}$),¹⁸ the excitation by the perpendicular laser gives a Doppler-

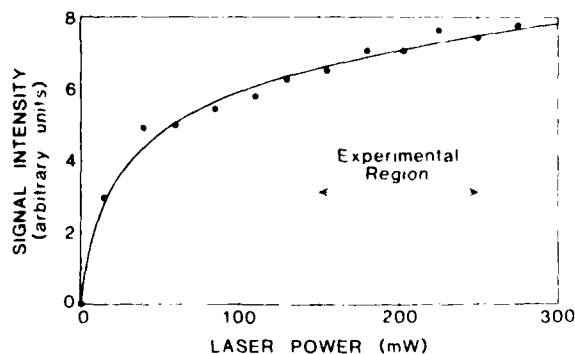


FIG. 5. Laser power dependence of the SDLIF signal. The solid circles represent experimental results.

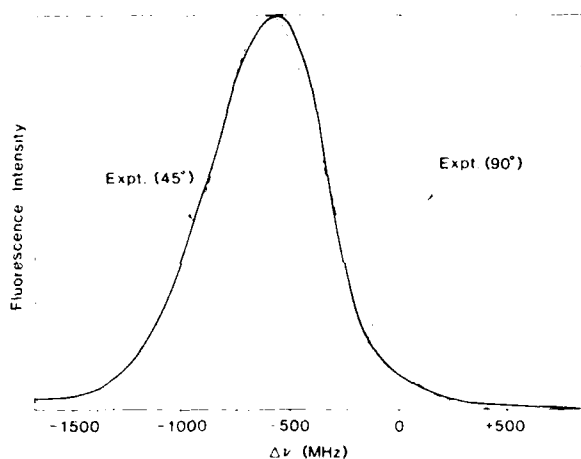


FIG. 6. A Doppler-shift spectrum of the Ba $1P^2-1S_1$ transition. The broken line is the calculated line profile using the Ba velocity distribution given by Eq. (10).

free signal, while the excitation by the laser at 45° provides a Doppler-shifted signal, as shown in Fig. 6. Note that the Ba atomic line shows several components due to different isotopes, some having hyperfine structure.¹⁹ By convoluting the Doppler-free line shape with the Doppler-shifted line shape, we obtained the (unnormalized) Ba beam velocity distribution²⁰ as

$$f(v_{Ba}) = (v_{Ba})^2 \exp[-(v_{Ba} - v)^2/\alpha^2], \quad (10)$$

where $v = 300 \text{ ms}^{-1}$ and $\alpha = (2kT/m_{Ba})^{1/2}$ at $T = 985^\circ\text{C}$.

III. RESULTS AND DISCUSSION

A. Rotational distribution of the BaI($v = 8$) product

Figure 7 shows the rotational distribution of the BaI($v = 8$) product produced in the Ba + HI reaction. The highest J observed here is 350.5. Thus, in order to probe more than 300 rotational levels, the single-mode laser must be scanned more than 25 cm^{-1} . In a given experiment, each rotational line is measured at least twice, and the average value is presented here. The measurements are performed at different times during an experiment, in an attempt to avoid possible systematic deviations due to, for example, a long-term variation of the Ba beam flux. The error bars given in Fig. 7 are associated with the following: (1) deviations of the measurements for each J ; (2) deviations of measurements for the adjacent ten rotational levels; (3) errors from the power normalization; and (4) errors involved in the slit function corrections. The error bars should be taken as being on the safe side.

A similar experiment was performed using a much weaker laser power ($\approx 20 \text{ mW}$) to test the effect of the laser power and detection scheme (flux or density) on the resulting distribution. The results of this experiment agreed with the one shown in Fig. 7 within experimental error.

B. Specific opacity function: No velocity dependence of reaction probability

From Eq. (8), it can be seen that the rotational distribution $P(J)$ provides information about the probability of reaction as a function of both v_{rel} and b . The distribution of $v_{rel} = |v_{Ba} - v_{HI}|$ can be calculated from the experimentally determined $f(v_{Ba})$, Eq. (10), and a Maxwell-Boltzmann distribution for the HI gas using a Monte Carlo simulation technique. The simplest treatment is to ignore any dependence of the reaction probability on relative collision velocity.

In order to determine the specific opacity function, $P_v(b)$, from the experimentally determined $P(J)$, we expand the specific opacity function $P_v(b)$ in terms of δ functions, as

$$P_v(b) = \sum_i a_i \delta(b - b_i), \quad (11)$$

where b_i is some impact parameter, and a_i is the weighting factor of b_i . For each member in the expansion, the corresponding rotational distribution $P_v(J)$ can be calculated by using Eq. (8), once the reactive velocity distribution is given. Thus, the observed rotational distribution is related to the calculated distribution by

$$P(J) = \sum_i a_i P_v(J). \quad (12)$$

Hence, the problem of obtaining the specific opacity function $P_v(b)$ is reduced to determining the expansion coefficients $\{a_i\}$ using a linear least-squares fitting method.

The observed and generated rotational distributions were first smoothed using a 15-point moving average, and then extrapolated to $J = 0.5$ and $J = 480.5$. The coefficients

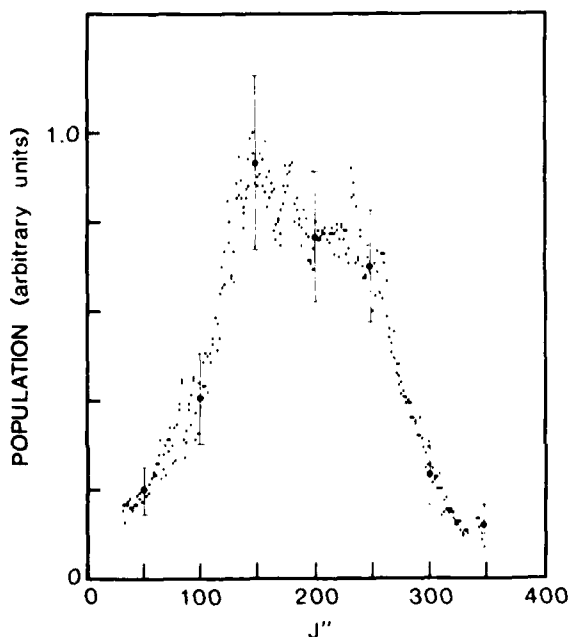


FIG. 7. The rotational distribution (unsmoothed) of the BaI product in $v = 8$ produced by the Ba + HI beam-gas reaction

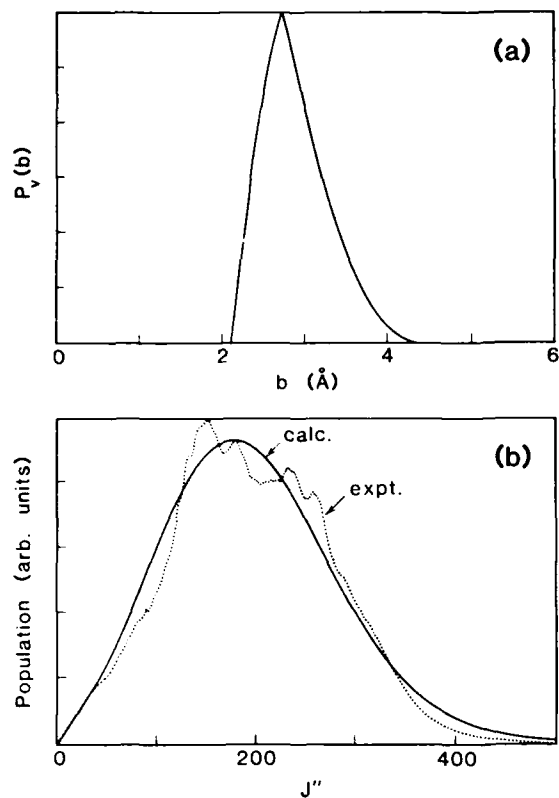


FIG. 8. (a) The specific opacity function for the Ba + HI \rightarrow BaI($v=8$) + H system, assuming there is no velocity dependence for the reaction. (b) The experimental (dot) and calculated (solid line) rotational distributions for the reaction studied using the specific opacity function shown in (a).

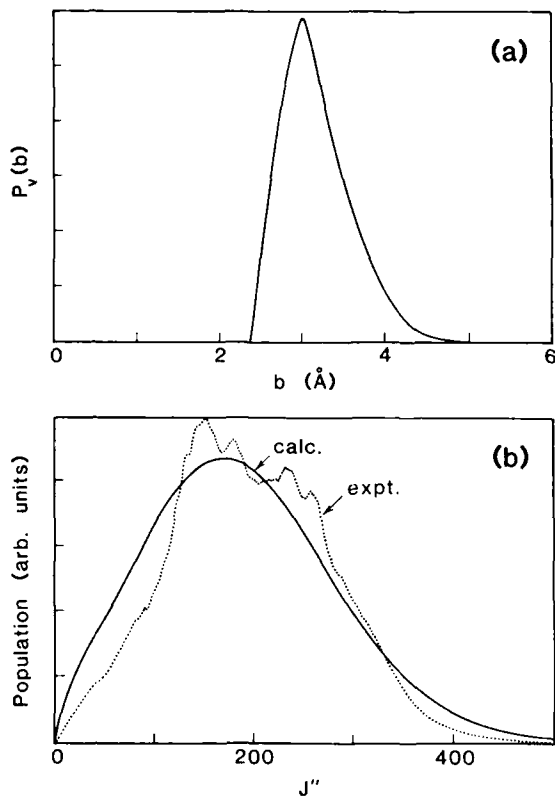


FIG. 9. (a) The specific opacity function for the Ba + HI \rightarrow BaI($v=8$) + H system, assuming that the reaction probability varies as $v_{\text{rel}}^{1/2}$. (b) The experimental (dot) and calculated (solid line) rotational distributions for the reaction studied using the specific opacity function shown in (a).

$\{a_i\}$ were computed by the least-squares method with the constraint that the coefficients must be positive.²¹ Since this procedure is extremely sensitive to the "noise," the resulting coefficients are smoothed using five-point moving average.

The "best-fit" specific opacity function obtained in this manner has a peak near 2.6 Å with a width of 1.0 Å (FWHM) as shown in Fig. 8(a). The smoothed observed and calculated rotational distributions are also compared in Fig. 8(b). The specific opacity function in Fig. 8(a) gives a remarkably good fit. Thus, it is concluded that for this model *only a limited range of impact parameters contributes to the formation of BaI($v=8$)*.

Very often the overall opacity function is stylized as a step function or a smoothly decreasing function of the impact parameter (see, e.g., Fig. 6.6 of Ref. 2). These simple models have been successful in describing impact parameter dependence in a previous experimental study²² on Rb + HBr. However, the experimentally determined opacity function reported here is specific to a particular product vibrational state, namely $v=8$, while the often-quoted opacity functions are *not* for a specific product vibrational state, but for all product states, and do not necessarily resemble the specific opacity functions.

C. Specific opacity function: Intrinsic velocity dependence of reaction probability

The simplest model, considered above, ignores any velocity dependence in the reaction probability. We consider next how the specific opacity function is modified if there is an intrinsic velocity dependence. We have investigated two cases, one in which the reaction probability varies as $v_{\text{rel}}^{1/2}$, the other as v_{rel}^0 . The resulting specific opacity functions are presented in Fig. 9 for the former case, and in Fig. 10 for the latter.

The shapes of these specific opacity functions are not very different from the specific opacity function with no velocity dependence discussed in the previous section. The significant difference is that the specific opacity functions shift their peaks toward small impact parameter as the velocity dependence is varied from v_{rel}^0 , v_{rel}^0 (no dependence), and $v_{\text{rel}}^{1/2}$. This can be explained as follows: if the collisions with the slower relative velocity are heavily weighted by $v_{\text{rel}}^{1/2}$, then the collisions with the larger impact parameters must have more probability to yield the same rotational distribution as produced by the v_{rel}^0 weighting. Whatever the exact form of the intrinsic velocity dependence is, we conclude

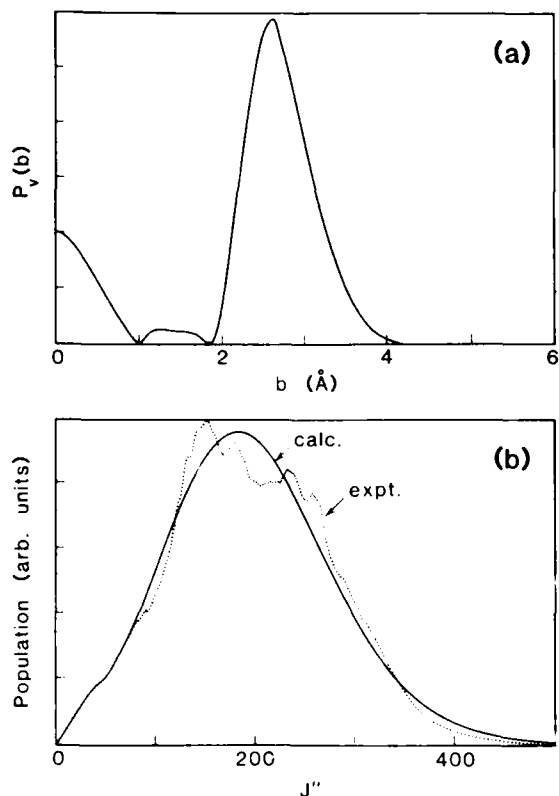


FIG. 10. (a) The specific opacity function for the Ba + HI + BaI($v = 8$) + H system, assuming that the reaction probability varies as v_{rel}^{-2} . (b) The experimental (dot) and calculated (solid line) rotational distributions for the reaction studied using the specific opacity function shown in (a).

that this type of velocity dependence has little effect on the specific opacity function for the reaction studied here.

D. Specific opacity function: Transmission velocity dependence of reaction probability

As a last model, we consider the situation where the reaction channel has an activation energy, i.e., only collisions with relative velocities greater than some threshold value lead to reaction (see Fig. 11). The procedure to calculate the probability for a trajectory to surmount the barrier is based on the "line-of-centers" model,^{1,2} and is described in the Appendix. In this model, we only consider the activation energy barrier for the system, and the energetic constraint on the relative velocity distribution is not included.

The Ba + HI reaction is only slightly exothermic. The excess energy available to the BaI reaction product is given by

$$E(\text{BaI}) = D_0^0(\text{BaI}) - D_0^0(\text{HI}) + E(\text{HI}) - E(\text{H}) + E_{\text{trans}} - E'_{\text{trans}}, \quad (13)$$

where E denotes an internal energy, D_0^0 the bond energy, and E_{trans} the translational energy of the reactants (double prime) or the products (single prime). For the reaction under study, $E(\text{Ba}) = 0$, $E(\text{HI}) = kT$, the average rotational

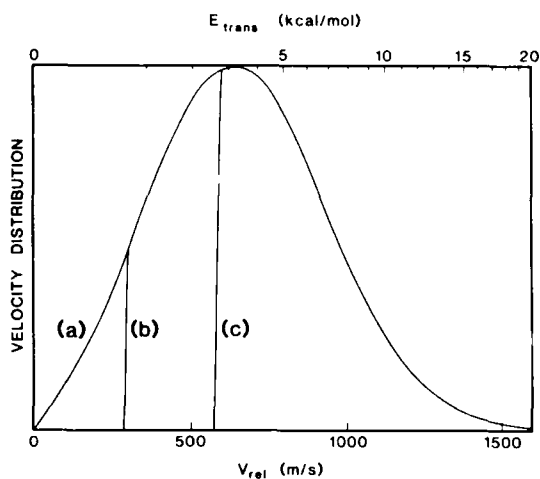


FIG. 11. The velocity distribution used for the analysis with the energy barrier set equal to (a) 0 kcal/mol, (b) 0.5 kcal/mol, and (c) 2.0 kcal/mol. Since the height of the centrifugal barrier varies with the impact parameter, the cutoff velocity changes as a function of b . A value of $b = 3 \text{ \AA}$ is used in preparing this figure.

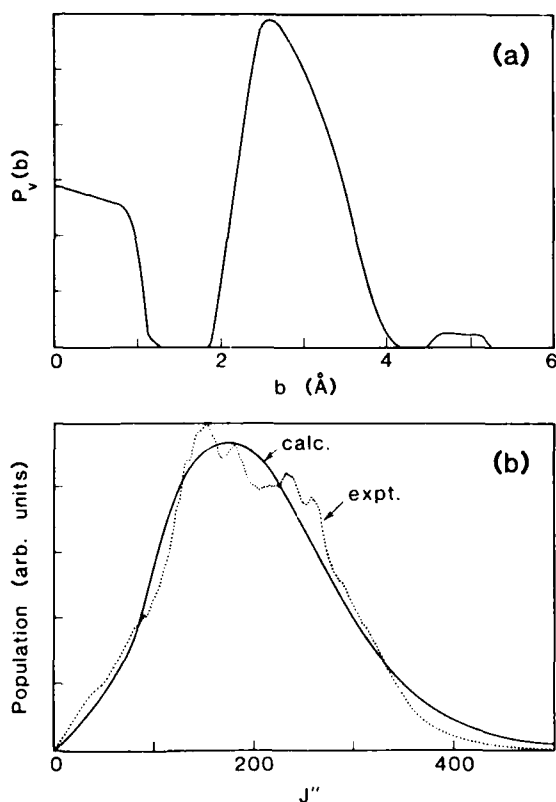


FIG. 12. (a) The specific opacity function for the Ba + HI + BaI($v = 8$) + H system, assuming that there exists an activation energy of 0.5 kcal/mol. (b) The experimental (dot) and calculated (solid line) rotational distributions for the reaction studied using the specific opacity function shown in (a).

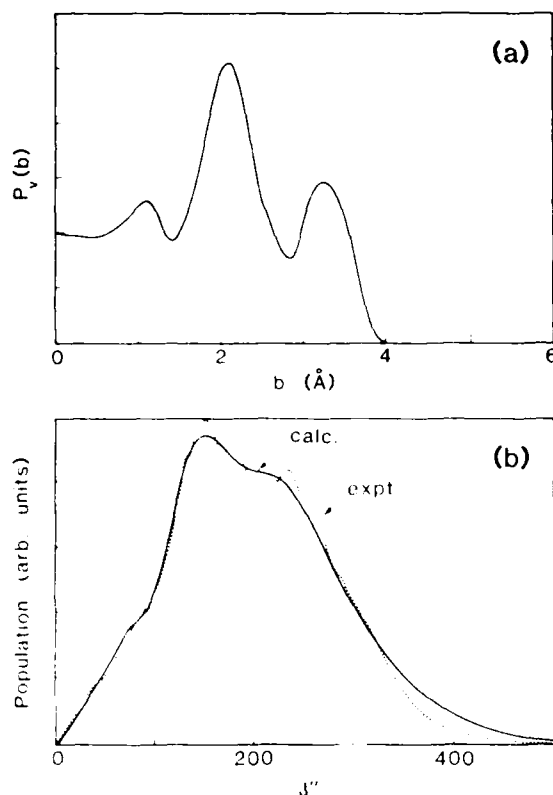


FIG. 13. (a) The specific opacity function for the Ba + HI ($\nu = 8$) + H system, assuming that there exists an activation energy of 2.0 kcal/mol. (b) The experimental (dot) and calculated (solid line) rotational distributions for the reaction studied using the specific opacity function shown in (a).

energy, $D_0(\text{HI}) = 70.4$ kcal/mol,²⁴ and $D_0^{\infty}(\text{BaI})$ has been variously reported as 71.4 ± 1.0 kcal/mol from a mass spectrometric thermochemical study,²⁴ 72.9 kcal/mol from a chemiluminescence study,²⁵ and less than 77.4 kcal/mol from a study of excited state predissociation.²⁶ We take the value $D_0^{\infty}(\text{BaI}) = 72.9$ kcal/mol but with the understanding that the dissociation energy is still not established. With this value

$$E(\text{BaI}) = 3.1 \text{ kcal/mol} + E_{\text{trans}} - E_{\text{trans}}, \quad (14)$$

However, about 3.4 kcal/mol is required to populate the $\nu = 8$ vibrational level.¹⁷ While we anticipate that E_{trans} is much less than E_{trans} because translational energy of the reactants appears primarily as rotational energy of the products, it appears nevertheless that the BaI ($\nu = 8$) channel might have a small energy deficit which might be made up by the translational energy of the reactants. Again this suggests the possibility of a small energy barrier in the reaction channel. This is expected to affect the opacity function in a way similar to how an activation energy barrier does.

Figures 12 and 13 show the specific opacity functions for the cases where the energy barrier is equal to 0.5 and 2.0 kcal/mol, respectively. As the energy barrier becomes higher, more of the slower velocities are rejected causing the reaction probability to increase at smaller impact parameters.

This tendency has already been noted in the previous section, but the effect of the transmission velocity dependence is much more pronounced than the intrinsic velocity dependence, mainly because all collisions with translational energy less than the activation energy barrier are unable to produce BaI ($\nu = 8$). Nevertheless, the specific opacity function does show a central peak near 2.6 Å suggesting that a small range of impact parameters are particularly effective in forming the BaI product in $\nu = 8$.

Mims, Lin, and Herm²⁸ have studied this reaction by measuring the BaI angular distribution produced under crossed-beam conditions. Their analysis indicated there is a translational energy barrier of 2.5 ± 1.0 kcal/mol. Since their analysis did not take into account the product vibrational and rotational excitation, we reanalyzed their angular distribution data. The results obtained indicated that the angular distribution is fairly insensitive to the translational energy barrier height and a moderate agreement can also be obtained by taking the Ba + HI barrier height to be zero. Siegel and Schultz²⁹ studied the Ba + HCl and Ba + HBr reactions at different collision energies and suggested that there is little or no activation energy in these analogous systems.

Because of the limited amount of information on the velocity dependence, we cannot determine presently the specific opacity function for this reaction system. It can be speculated that the intrinsic velocity dependence has little effect on the specific opacity function, while the possible existence of an activation energy barrier and the uncertainty in the exoergicity of the reaction could greatly alter the form of the derived specific opacity function. Clearly further experimental work is needed in order to establish the reaction cross section as a function of the collision energy.

ACKNOWLEDGMENTS

We are grateful to A. E. DePristo for suggesting a least-squares procedure for extracting $P_v(b)$ from the rotational distribution, to J. L. Durant for his help in taking a spectrum shown in Fig. 1, and to D. Yen for his help in the early stages of this study. We also warmly thank the referee for his valuable comments. This work was supported in part by the National Science Foundation under NSF CHE 85-05926 and the Air Force Office of Scientific Research under AFOSR F49620-85-C-0021. RNZ thanks support through the Shell Distinguished Chairs Program, funded by the Shell Companies Foundation, Inc.

APPENDIX

In order for a trajectory to reach a transition state, sufficient translational energy must be provided to surmount the energy barrier. The latter consists of an activation energy, E_0 , and a centrifugal energy, E_c , i.e.,

$$E_{\text{trans}} = E_0 + E_c, \quad (\text{A1})$$

where E_{trans} equals $\mu v_{\text{rel}}^2/2$. The centrifugal energy is expressed using Eq. (8) as

$$\begin{aligned}
 E_c &= \frac{1}{2\mu r^2} J^2 \\
 &= \frac{\mu v_{rel}^2}{2} \frac{b^2}{r^2} \\
 &= \frac{b^2}{d^2} E_{trans}, \quad (\text{A2})
 \end{aligned}$$

where we have assumed that the maximum of the energy barrier lies at d

From Eqs. (A1) and (A2), we obtain

$$E_{trans} \geq E_0(1 - b^2/d^2)^{-1}. \quad (\text{A3})$$

Thus, because of the line-of-centers functionality,^{1,2} the minimum translational energy needed to reach a transition state becomes a function of the impact parameter.

In the actual computation, the value of d is set to 6 Å, and the velocity dependence around the cutoff velocity is replaced by a gradually decreasing function rather than one having a sharp cutoff.

¹The boiling point is -35.38°C ; see *Handbook of Chemistry and Physics* (Chemical Rubber, Cleveland, 1984).

²H. W. Cruse, P. J. Dagdigan, and R. N. Zare, *Faraday Discuss. Chem. Soc.* **55**, 277 (1973).

³M. A. Johnson, C. R. Webster, and R. N. Zare, *J. Chem. Phys.* **75**, 5575 (1981).

⁴J. R. Waldeck, C. Noda, J. S. McKillop, and R. N. Zare (in preparation).

⁵C. Linton, *J. Mol. Spectrosc.* **69**, 351 (1978); M. Dulick, P. F. Bernath, and R. W. Field, *Can. J. Phys.* **58**, 703 (1980).

⁶I. Kovács, *Rotational Structure in the Spectra of Diatomic Molecules* (Elsevier, New York, 1969).

⁷M. G. Prisant, C. T. Rettner, and R. N. Zare, *J. Chem. Phys.* **81**, 2699 (1984), and references therein.

⁸J. Allison, M. A. Johnson, and R. N. Zare, *Faraday Discuss. Chem. Soc.* **67**, 124 (1979).

⁹R. I. Altkorn and R. N. Zare, *Annu. Rev. Phys. Chem.* **35**, 265 (1984).

¹⁰W. Demtröder, *Laser Spectroscopy*, 2nd ed. (Springer, Berlin, 1982).

¹¹C. E. Moore, *Atomic Energy Levels*, Natl. Bur. Stand. (U. S. GPO, Washington, D.C., 1971), Vol. III.

¹²P. E. G. Baird, R. J. Brambley, K. Burnett, D. N. Stacey, D. M. Warrington, and G. K. Woodgate, *Proc. R. Soc. London Ser. A* **365**, 567 (1979).

¹³Since the laser power is very low, laser-induced fluorescence works as a density detector. Thus, the velocity distribution function contains a v^2 factor instead of a v^3 factor which appears in the flux distribution.

¹⁴D. W. Marquardt, *J. Soc. Ind. Appl. Math.* **11**, 431 (1963).

¹⁵J. E. Mösch, S. A. Safran, and J. P. Toennies, *Chem. Phys. Lett.* **29**, 7 (1974).

¹⁶K. P. Huber and G. Herzberg, *Molecular Spectra and Molecular Structure. IV. Constants of Diatomic Molecules* (Van Nostrand Reinhold, New York, 1979).

¹⁷P. D. Kleinschmidt and D. E. Hildenbrand, *J. Chem. Phys.* **68**, 2819 (1978).

¹⁸R. C. Estler and R. N. Zare, *Chem. Phys.* **28**, 253 (1978).

¹⁹M. A. Johnson, Ph.D. thesis, Stanford University, 1983.

²⁰ $\sigma = 152.60 \text{ cm}^2$ reported by M. M. Patel (private communication, 1975).

²¹C. A. Mims, S.-M. Lin, and R. R. Herm, *J. Chem. Phys.* **57**, 3099 (1972).

²²A. Siegel and A. Schultz, *J. Chem. Phys.* **72**, 6227 (1980).

¹R. D. Levine and R. B. Bernstein, *Molecular Reaction Dynamics* (Oxford University, New York, 1974).

²R. B. Bernstein, *Chemical Dynamics via Molecular Beam and Laser Techniques* (Oxford University, New York, 1982).

³D. R. Herschbach, *Adv. Chem. Phys.* **10**, 319 (1966).

⁴N. H. Hijazi and J. C. Polanyi, *J. Chem. Phys.* **63**, 2249 (1975); *Chem. Phys.* **11**, 1 (1975).

⁵C. T. Rettner, I. Woste, and R. N. Zare, *Chem. Phys.* **58**, 371 (1981).

⁶M. A. Johnson, C. Noda, J. S. McKillop, and R. N. Zare, *Can. J. Phys.* **62**, 1467 (1984).

⁷J. S. McKillop, Ph.D. thesis, Stanford University, 1986.



Accession	
NTIS	✓
DTIC	
Unann	
Just	
By	
Dist	
Avail	
Dist	
A-1 20	



FILMED
2=8